International Journal of Power Electronics and Drive System (IJPEDS)
Vol. 10, No. 2, June 2019, pp. 1102~1109
ISSN: 2088-8694, DOI: 10.11591/ijpeds.v10.i2.pp1102-1109

Morphology and magnetic properties of lanthanum (La^{3+}) substituted manganese, chromium nano ferrites

Hayder Abdulameer Abbas, Adnan Hussein Ali, Ban Mohammad Hasan
Technical Instructors Training Institute, Middle Technical University, Iraq

Article Info

Article history:

Received Nov 27, 2018
Revised Jan 1, 2019
Accepted Mar 3, 2019

Keywords:

La^{3+} substitution,
Nano ferrites,
Structural and magnetic properties

ABSTRACT

Several studies have been carried out to investigate the effect of Lanthanum (La^{3+}) ion substitution on the structural and magnetic properties of manganese-chromium (Mn-Cr) ferrite of chemical formula Mn La_xCr Fe_2O_4(x=0.0, 0.25 and 0.5). Such studies have made efforts to improve the magnetic and structural properties of manganese-chromium (Mn-Cr) ferrite by using lanthanum substituted nano ferrites and then synthesized using the sol-gel method and annealed at a temperature of 700°C. The changes that occurred in the structure of the nano ferrites as a result of lanthanum substitution were identified using X-ray diffraction (XRD). Based on Debye-Scherrer equation, the XRD data were used in measuring the particle sizes of different diffraction and average crystallite size by means of Fourier Transform infrared spectroscopy (FTIR). In analyzing the morphology of the nano ferrites, scanning electron microscopy (SEM) was used, elemental compassion was studied using energy dispersive X-ray spectroscopy (EDAX), and the average particle diameter was determined using Transmission electron microscopy (TEM) studies. FTIR spectral analysis of the prepared samples under investigations revealed the formation of a single phase spherical particles. Two important absorption bands were observed; one (v_1) around 556 cm^{-1}, which is attributed to the intrinsic vibrations of tetrahedral complexes, while the other low frequency band (v_2) was around 430 cm^{-1}, and attributed to octahedral complexes.

Corresponding Author:

Hayder Abdulameer Abbas,
Technical Instructors Training Institute
Middle Technical University, Baghdad, Iraq.
Email: haeder_abid@yahoo.com

1. INTRODUCTION

Ferrites are ferrimagnetic semiconductors, which have led to the emergence of a new research area in the physics of material science. They are also regarded as high resistivity ferrites that can be used in producing different ferrites [1]. Ferrite materials are considered as vital materials in the production of several electromagnetic devices such as Isolators, converters, inductors, phase shifters, circulators and electromagnetic wave absorbers [2]. Extensive studies have been conducted on spinel ferrites because they are easy to synthesize and can be used for a wide range of technological and industrial applications. It is important to synthesize Nano ferrites such as metallic spinel ferrites that are characterized by a low size distribution; this is important because they possess notable magnetic and electrical properties [3]. More so, they are widely used in practical applications in advanced information technologies like, medical diagnostics, magneto caloric refrigeration, etc. There are a number of factors that can affect the magnetic properties of Nano Ferrite's [4], and some of them include; chemical composition, type of substituent, grain size, preparation method, distribution of cation in the tetrahedral (A) and octahedral [B] sites, doping, voids and surface layers. Different methods like co-precipitation, sol-gel method have been used in synthesizing Electro & Magnetic Nano ferrites with general structure MFe_2O_4. Several attempts have been made by researchers to

improve the quality of ferrites through the addition of the same appropriate nonmagnetic/diamagnetic contaminations with varying valence state of the A and B sites includes Lanthanum (La^{3+}) [5]. Lanthanum, which is regarded as the 2nd most robust and lightest scarce earth element among the lanthanide category, possesses a unique quality in comparison to other scarce earth element like simple electronic spectra which is more useful in experimental analysis [6]. Therefore, the demand for La^{3+} is high as it can be used in crucial applications such as NiMH batteries, which are presently used in all hybrid-electric vehicles [7, 8].

Manganese ferrites, which possess a cubic spinel structure, are popularly known as magnetic ferrites that are used in various technological applications. These ferrites have properties that are dependent on morphology, size and composition, which have a strong correlation with the preparation conditions [9, 10]. Presently, the use of various methods of synthesis is being employed in synthesizing the different compositions of manganese ferrites [11, 12]. However, the sol-gel method of synthesis is more robust due to the high level of compositional uniformity it offers within a short period of processing and at a very low temperature for the synthesis of nano ferrites [13].

According to G. Kumar, rare earth oxides serve as good electrical insulators with high electrical resistivity. Thus, the magnetic and electrical properties of spinel ferrites can be modified if the appropriate rare earth cation is selected [14, 15]. When the parent ferrite is substituted with selected rare earth ions, the morphology becomes transformed in different ways [16, 17].

For the greatest of our information, there aren't various research analysis focused on the comprehensive structural and morphological investigation of the lanthanum La^{3+} ion substitution into the Mn-Cr-Fe_2O_4. Therefore, this current work is focusing on investigating the effect of rare earth lanthanum ion substitution on the structural, magnetic and morphological properties of of Mn-Lax-Cr-Fe_2O_4 utilizing a sol-gel method. The structural, magnetic and morphological properties of synthesized nanoparticles were examined and analysed. Therefore, this study focuses on studying the effect of La^{3+} substitution in Mn-Cr-Fe_2O_4. The nanoparticles of Mn-Lax-Cr-Fe_2O_4 are synthesized using the sol-gel method. A discussion on the structural and magnetic properties of the samples that have been synthesized is given subsequently.

2. EXPERIMENTAL EQUIPMENTS

2.1. Material and method

All chemicals and solvents used in the experiments were AR grade, and purchased from Merck Co.Pvt Ltd and Sd. The chemicals used were fine and needed no further purification. The stoichiometric amounts of metal nitrates viz, [$La(NO_3)_3 \cdot 6H_2O$], Ferric Nitrate [$Fe(NO_3)_2$ $9H_2O$], Chromium Nitrate [$Cr(NO_3)_2 9H_2O$], Citric acid ($C_6H_8O_7.H_2O$) used as starting materials for the synthesis.

2.2. Synthesis of nanoparticles

The required quantity of metal nitrates were dissolved in a little amount of distilled water and afterwards mixed together. An addition of an aqueous solution of citric acid was made to the mixed metal nitrate solution (with and without Lanthanum nitrate). Afterwards, an addition of ammonia solution was also made to the mixture and it was constantly stirred with a neutral pH of (7.0) maintained. The solutions were heated at a temperature of 90ºC with continuous stirring so as to eliminate the extra solvent. In order to ignite the gel, the temperature was increased to 200°C. A powder-like substance was obtained from the dried gel, which was completely burnt in a self-propagating combustion manner. An Agate Mortar and Pestle was used in grinding the burnt powder so as to obtain a fine ferrite powder. Lastly, a temperature of 700°C was applied to the burnt powder in order to calcinate in the air for 2 hours. Afterwards the powder was allowed to cool own in room temperature.

2.3. Equipments characterization

2.3.1.X-ray diffraction

The use of SCINTAG X'TRA AA85516 (Thermo ARL) X-ray diffractometer alongside Peltier cooled Si solid detector was employed in performing the XRD analysis of the prepared samples. Monochromatized Cu K_a (λ=1.5405 Å) was used as the radiation. Diffraction patterns were collected at 45 kV– 40 mA, at 0.02°C step and count time of 0.400 sec over a range of 10.00–80.0 (2θ), at a step scan rate of 3.00 min^{-1} and the crystallite size (D) is calculated from X-ray line broadening of the (311) diffraction peak using the well-known Debye-Scherer's formula:

$$D = \frac{0.9\lambda}{\beta \cos\theta} \quad (1)$$

where β represents the full-width at half-maxima of the strongest intensity diffraction peak (311), λ denotes the wavelength of the radiation, and θ the angle of the strongest characteristic peak.

The following equation was used in calculating the X-ray density (ρ_x):

$$\rho x = \frac{8M}{Na^3} \quad (2)$$

where the molecular weight is denoted by M , N Avogadro's number represented by (gm) (per mol) and a the lattice parameter in angstrom.

Based on the high intense peak of (311) of the XRD pattern, the value of lattice parameter a was determined using equation (3) below. The values are contained in Table 1.

$$a = \frac{d_{hkl}}{(\sqrt{h^2+k^2+l^2})} \quad (3)$$

where a is lattice constant d_{hkl} is inter-planar distance for hkl plane.

2.3.2.FTIR spectroscopic analysis

Fourier Transform Infrared Spectroscopy (FTIR) was used in examining the adsorbents. The preparation of the samples was carried out by mixing 1 mg of powdered carbon with 500 mg of KBr (Merck-spectroscopy quality) in an agate mortar. The mixture which was obtained was then pressed under a pressure of 5 tones/ cm^2 for about 5 minutes, and at 10 tones/ cm^2 for 5 minutes under vacuum. The measurements for the spectra were performed within the range of 4000 to 400 cm^{-1} on a JASCO-FTIR-5300 model.

2.3.3.SEM-EDX analysis

A two-sided adhesive carbon tape was used to stub the surfaces of the powdered carbonaceous materials. Coating of the samples was done within a period of 120sec with 20mA using a platinum coater (JOEL Auto fine coater model, JFC –1600); a thin layer of platinum was deposited on the samples. The use of SEM JEOL model, JSM-5600 alongside an EDX analyzer was employed in recording the microphotographs of the samples with an accelerating voltage of 5 kV, at high vacuum mode. The equipment has a maximum magnification capacity of 300,000 times with a resolution of 3 nm. Different magnifications were used for the samples under study.

2.3.4.TEM analysis

First of all, the ferrite sample was sonicated (Vibronics VS 80) for 5 minutes and deposited on carbon coated copper grids, after which, the solvent was exposed to infra light for 30 minutes so as enable evaporation. The use of Philips model CM 20 instrument, which was operated at an accelerating voltage of 200 kV was employed in TEM measurements.

The magnetic properties of the samples were examined using Hysteresis Tracer in the field of 10 kOe at room temperature.

3. RESULTS AND DISCUSSION

3.1. XRD studies

The classic patterns of X-ray diffraction of Mn La_x Cr Fe_2O_4 (where X=0.0, 0.25, 0.50) Nano ferrites and those annealed at 700°C are shown in Figure 1. The crystalline phase and the identification of peaks was carried out by comparing the '*d*' spacing with that of JCPDS data of $MnFe_2O_4$ and $CrFe_2O_4$. The formation of a single phase a face centred cubic (fcc) spinel structure was confirmed through the main lattice planes (220), (311), (222) (400), (422), (511), (440), (533), (622) and (444). This indicates that the the La^{3+} ions have been completely dissolved into the spinel lattice of Mn-Cr ferrite.

Based on the line broadening of the most intense peak (311) of the plane of the spinel structures, the average crystallite size of the prepare samples were calculated using the Scherrer equation[8]. It is observed that a decrease in the particle size caused an increase the concentration of La^{3+} cation; TEM analysis was also used to confirm this result.

There is a possibility of the Fe^{3+} cations being replaced by the lanthanum ions in the octahedral sites, which can be concluded from the uniformity of the lattice constant values for the different concentrations of La^{3+} ions. As the content of La^{3+} ion increases, the peaks become broader. This is an indication of a constant reduction in particle size, which is marked from the values of crystallite sizes contained in Table 1. These results are similar with that previous studies studies.

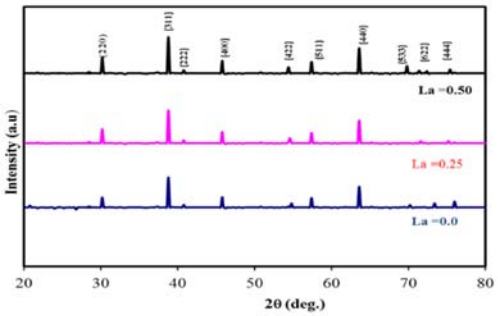

Figure 1. X-ray diffraction patterns of Mn La_x Cr Fe_2O_4 (where X=0.0, 0.25, 0.50) Nano ferrites

Table 1. Crystal & magnetic parameters of Mn-Cr ferrites for various concentrations of La^{3+} ion

Concentration of La^{3+} ion	Crystallite size (nm)	Lattice constant (Å)	X-ray density (g cm^{-3})	Magnetization (emu/g)	Coercivity (Oe)	Retentivity (emu)
0	19.2547	8.231	6.254	21.8471	14025.21	17.264
0.25	18.0698	8.264	6.984	20.6487	17245.34	16.257
0.5	18.1578	8.198	7.021	18.9842	16824.57	16.128

3.2. FTIR studies

In order to study the bonding of the metal-oxygen in the prepared Nano ferrite samples, the use of Fourier transform infrared (FTIR) was employed. As seen in Figure 2, the FTIR spectra of the prepared ferrite nano particles were measured within the frequency range of 700cm^{-1} to 400 cm^{-1}. The formation of the spinel structure of Mn-La-Cr ferrite system was confirmed by FT-IR analysis. There are two notable absorption bands (ν_1 and ν_2) in the wavenumber ranging from 700 to 400 cm^{-1}. It was observed that these absorption bands correspond to the stretching vibration of the tetrahedral and octahedral sites, which occurred around 550 to 555cm^{-1}, respectively as seen in Table 2. The absorption bands indicate the unique characteristics of spinel ferrites in single phase. The variance between ν_1 and ν_2 is attributed to the changes that occurred in the bond length of Fe-O at the Octahedral and Tetrahedral sites. It can be observed from the table that the range of the high frequency band (ν_1) is from 551 to 555cm^{-1}. More so, it was also observed that the substitution of La^{3+} resulted in significant change in the ν_2 band corresponding to octahedral site. Based on observation, the ν_2 band (octahedral site) ranges from 460 to 466 cm^{-1} with a subsidiary band ν_3 in the range of 432 and 428 cm^{-1}, for two samples except for pure Mn-Cr ferrite. This result can be attributed to John-Teller distortion caused by La^{3+} doping as reported by Mamilla Lakshmi et al. Figure 2 shows that an increase in the content of La^{3+} caused the values to move to a lower-frequency side. Furthermore, it was observed that an increase in the concentration La^{3+} caused the absorption band to be slightly broadened. The substitution of Fe^{3+} ions by La^{3+} ions could be responsible for this occurrence.

Table 2. FTIR parameters of Mn La_x Cr Fe_2O_4 (where X=0.0, 0.25, 0.50) nano ferrites

Ferrite Composition	ν_1(cm^{-1})	ν_2(cm^{-1})	ν_3(cm^{-1})
Mn La_0 Cr Fe_2O_4	551.64	432.77	not identified
Mn $La_{0.25}$ Cr Fe_2O_4	553.57	466.44	428.19
Mn $La_{0.50}$ Cr Fe_2O_4	555.49	460.98	432.05

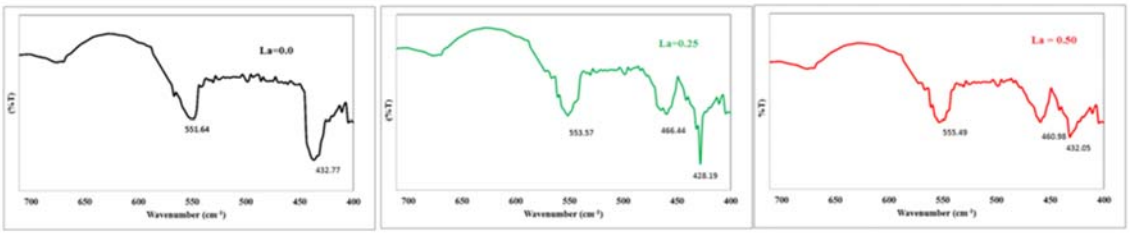

Figure 2. FTIR spectra of Mn La_x Cr Fe_2O_4 (where X=0.0, 0.25, 0.50) nano ferrites

3.3. SEM–EDX analysis

In order to study the surface morphology of the prepared nano ferrites, the use of scanning electron microscope (SEM) was employed. The result of the analysis is contained in Figure 3(a-c). The electron micrographs showed that the material is basically made up of some irregular cubic or rod-like particles in pure Mn-Cr ferrite (Figure 3(a)), and as the concentration of the La^{3+} increases, an increase also occurs in the agglomeration of these particles. It can be assumed that the nature of the exterior of these agglomerates is due to the chemical reaction in the process of sintering. The bonding of these agglomerates can be attributed to relatively weak Vander Waals bonds or even magnetic forces. For lanthanum compositions, well-crystallized solid grains of irregular shapes alongside small micro pores were observed. The incessant reduction in grain size, which occurs with the La^{3+} substitution, may be due to the fact that lanthanum ions possess large ionic radii than that of Iron (0.64 Å), and therefore, demonstrate limited solubility in spinel lattice, which in turn prevents the growth of grain as well as the decrease in the size of grain.

EDS was used in determining the sample composition, and the pattern that was obtained is presented in Figure 3(a-c) (right side). The presence of Mn, Fe, Cr, O and La was observed in the specimen (except in Figure 3(a); no other impurities were found in the sample.

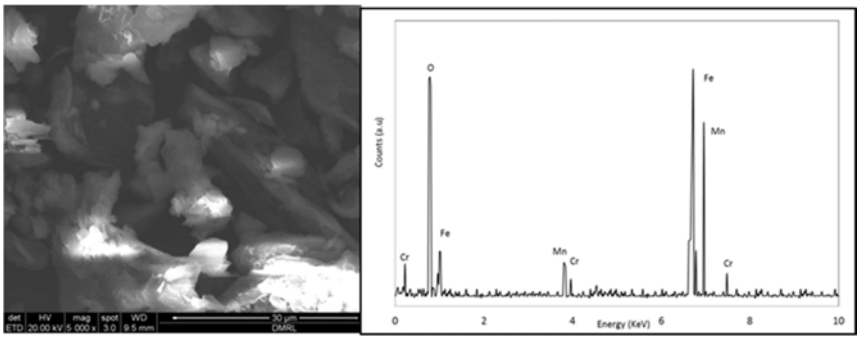

Figure 3(a). SEM-EDX spectra of Mn La_0 Cr Fe_2O_4

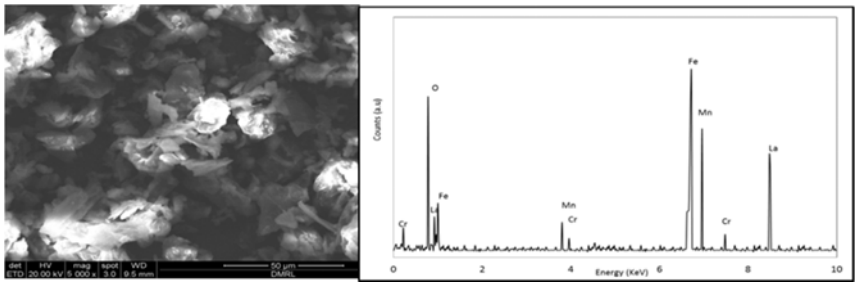

Figure 3(b). SEM-EDX spectra of Mn $La_{0.25}$ Cr Fe_2O_4

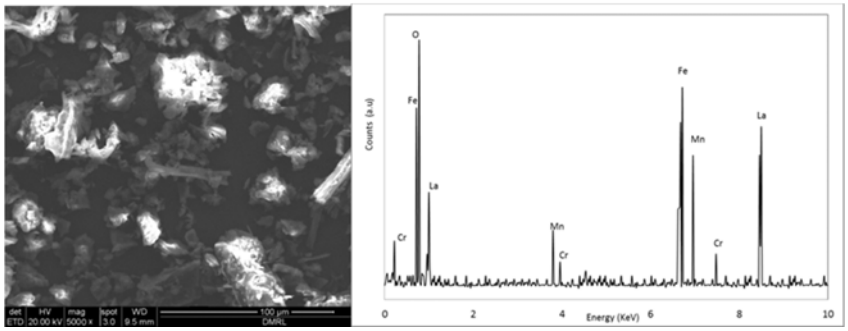

Figure 3(c) SEM-EDX spectra of Mn $La_{0.50}$ Cr Fe_2O_4

3.4. TEM analysis

Based on the TEM analysis performed on three nano ferrite sample, the TEM micrographs show that high level of agglomeration occurred in the particles as a result of the interfacial surface tension as reported in the review of literature. It can be observed that majority of the nanoparticles appeared slightly agglomerated with a shape that is almost spherical; this is shown in (Figure 4(a-c)). More so, as the concentration of lanthanum ion increased, a decrease occurred in the average particle size obtained from TEM such as; 19.18 nm (La=0.0), 18.72 nm (La=0.25) and 18.545 (La = 5.0). Similar pattern was also obtained from XRD studies.

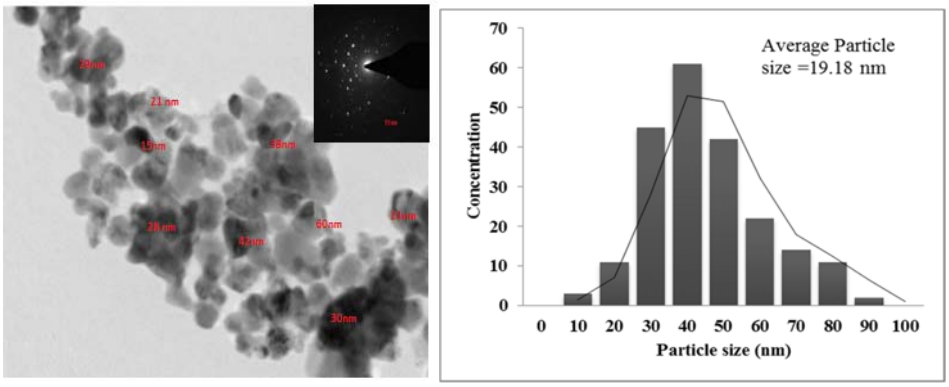

Figure 4(a). TEM images (left) of Mn La_0 Cr Fe_2O_4 and particle size distribution (right)

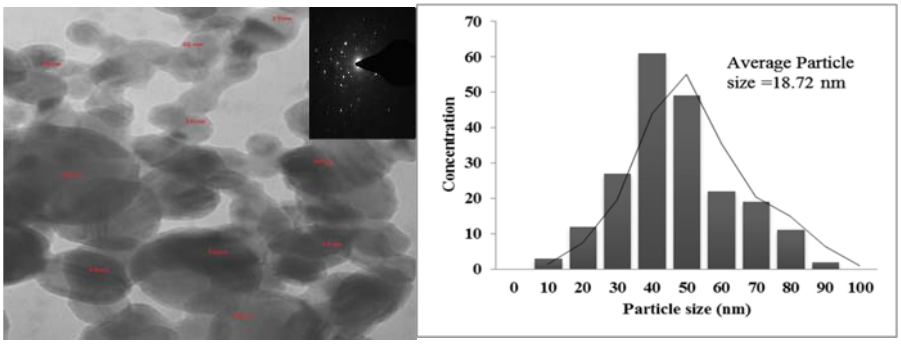

Figure 4(b). TEM images (left) of Mn $La_{0.25}$ Cr Fe_2O_4 and particle size distribution (right)

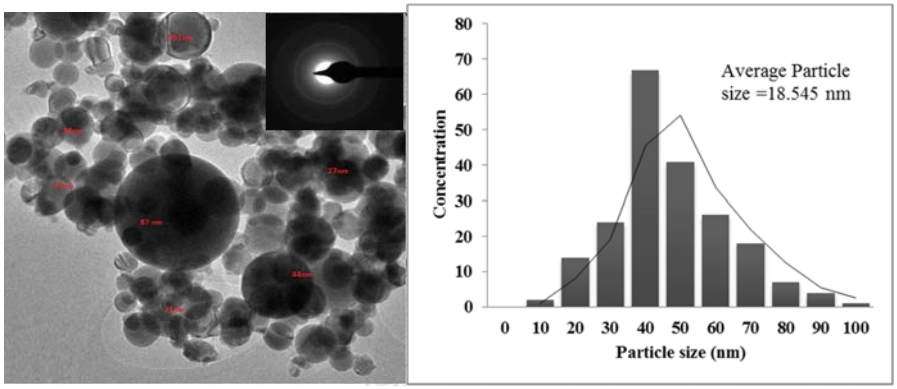

Figure 4(c). TEM images (left) of Mn $La_{0.5}$ Cr Fe_2O_4 and particle size distribution (right)

3.5. Magnetic properties

In order to calculate the magnetic parameters of the prepared nano ferrite samples, the use of vibrating sample magnetometer (VSM) was employed; the VSM was used within the range of 5000 Oe, where the magnetic behaviour of the samples was demonstrated. As contained in figure 5, the measurements from the VSM were used in plotting the hysteresis loops, from which the calculation of the values of saturation magnetisation for the various compositions $Mn\,La_x\,Cr\,Fe_2O_4$ (x=0.0, 0.25 and 0.50) was performed and represented graphically in Figure 5 and tabulated in Table 1. Figures 5 and 6 show the difference in the saturation magnetisation of the composition. The hysteresis loops revealed that for the values of (x= 0.0, 0.25 0.50) there was no complete saturation of samples. The result clearly indicates that the substitution of lanthanum caused a decrease in the saturation magnetization. The site occupancy of the cations as well as the alteration in the exchange effects caused by the substitution of lanthanum can be used in explaining this decrease.

The major contributors of the magnetic properties are the'Fe^{3+} ions, which occupy the 'B' sites in the inverse spinal lattice. The pragmatic nature of La^{3+} is attributed to the absence of unpaired electrons. It was observed the substitution of La^{3+} resulted in a significant decrease in coercivity. This theory posits that the coercivity is influenced by factors such as magneto crystalline anisotropy, micro strain, size distribution, magnetic particle morphology and magnetic domain size[11].

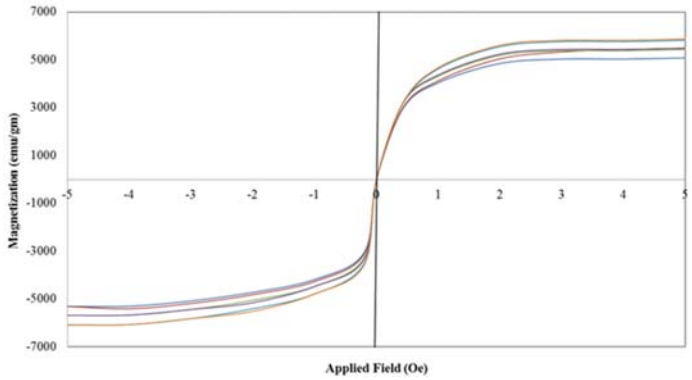

Figure 5. Hysteresis loops of manganese chromium ferrite for various La^{3+} concentrations

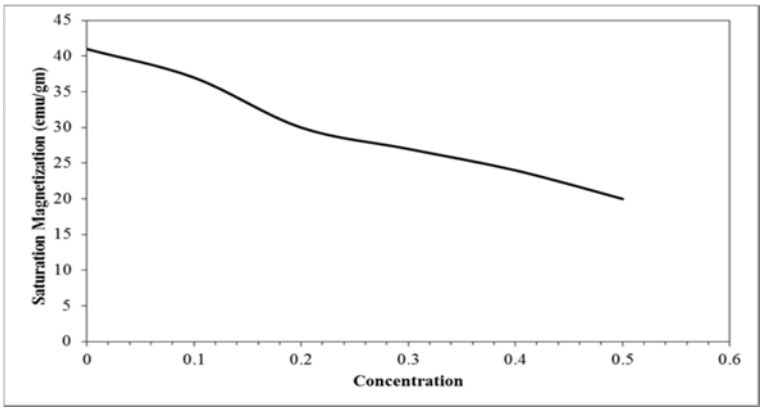

Figure 6. Plot of Magnetization Vs Concentration

4. CONCLUSION

The results of the experimental investigations revealed how Lanthanum doping affects the properties of spinel Lanthanum substituted Mn-Cr ferrites. The use of sol-gel method was employed in preparing the samples used in this study. Also, the magnetic and structural measurements were performed through the

process of sintering at a temperature of 700ºC. The presence of all characteristic reflections was confirmed by the X-ray diffraction results (220), (311), (222), (400), (422), (511), (440), (222), (533), (622), and (444), which confirmed the formation of single phase, cubic spinel structure. The substitution of La^{3+} led to a decrease in the crystallite size and lattice. The formation of the spinel structure with strong Metal oxygen adhesion was confirmed using the FTIR spectrum of the Nano crystal that was synthesized. The nature of the fused grain possessing intergranular diffusion in Mn La_x Cr Fe_2O_4 (where X=0.0, 0.25, 0.50) Nano ferrites were observed through the SEM images. It was observed that the three samples used in this study demonstrated 'S' like shape hysteresis curve. As the La^{3+} substitution increased, the decrease occurred in the magnetic parameters. The continuous increase in the La^{3+} concentration brought about a decrease in the crystallite size as well as in the saturation magnetization.

REFERENCES

[1] V. G. Harris, A. Geiler, Y. J. Chen, S, et al., "Recent Advances in Processing and Applications of Microwave Ferrites", *J. Magn. Mater*, 321: 2035; 2009.

[2] S. Suder, B.K. Srivastava, A. Krisnamurty, *Ind. J. Pure Appl. Phys*. 42 (2004) 366.

[3] Humphries M. "Rare Earth Elements: The Global Supply Chain", DIANE Publishing Company; 2010.

[4] S. Yáñez-Vilar, M. Sánchez-Andújar, C. Gómez-Aguirre, J. Mira, M. A. Seňaís-Rodríguez, and S. Castro-García, "A simple solvothermal synthesis of MFe2O4(M = Mn, Co and Ni) nanoparticles," *Journal of Solid State Chemistry*, vol. 182, no. 10, pp. 2685–2690; 2009

[5] D. Zhang, X. Zhang, X. Ni, J. Song, and H. Zheng, "Low-temperature fabrication of $MnFe_2O_4$ octahedrons: magnetic and electrochemical properties," *Chemical Physics Letters*, vol. 426, no. 1–3, pp. 120–123, 2006.

[6] Q. Zhang, M. Zhu, Q. Zhang, Y. Li, and H. Wang, "Fabrication and magnetic property analysis of monodisperse manganese-zinc ferrite nanospheres," *Journal of Magnetism and Magnetic Materials*, vol. 321, no. 19, pp. 3203–3206, 2009

[7] Gagan Kumar, Jyoti Shah, R. K. Kotnala, Pooja Dhiman, Ritu Rani, Virender Pratap Singh, Godawari Garg, Sagar E. Shirsath, Khalid M. Batoo, M. Singh. "Self-ignited synthesis of Mg-Gd-Mn nanoferrites and impact of cation distribution on the dielectric properties". *Ceram. Inter*. 2014, 40, 14509-14516

[8] Adnan H. Ali, Ali A. A.,"Efficiency Performances of Two MPPT Algorithms for PV System With Different Solar Panels Irradiancess", *International Journal of Power Electronics and Drive Systems (IJPEDS)*, Vol 9, No 4, pp. 1755-1764, December 2018.

[9] Ahmad, A., Bae, H., & Rhee, I.. "Highly stable silica-coated manganese ferrite nanoparticles as high-efficacy T2 contrast agents for magnetic resonance imaging". *AIP Advances*, 8(5), 055019, 2018.

[10] Krishna, K.R., Ravinder, D., Kumar, K.V. and Lincon, C.A. "Synthesis, XRD & SEM Studies of Zinc Substitution in Nickel Ferrites by Citrate Gel Technique". *World Journal of Condensed Matter Physics*. 2, 153-159; 2012.

[11] M. Raghasudha, D. Ravinder, and P. Veerasomaiah, "Effect of Cr Substitution on Magnetic Properties of Mg Nanoferrites Synthesized by Citrate-Gel Auto Combustion Method," *Journal of Chemistry*. 2013.

[12] Sopan M. Rathod, Sarang S. Bhosale, Pratikkumar K. Zagade, ,Datta B. Pawar,Ashok B. Shinde, "Synthesis and Characterizationof La3+ Doped Ni NanoFerriteby Sol-Gel Method", *Bionano Frontier*, Vol. 8 (3) December 2015

[13] Lakshmi, M., Kumar, K. and Thyagarajan, K. "Structural and Magnetic Properties of Cr-Co Nanoferrite Particles". *Advances in Nanoparticles*, 5, 103-113; 2016.

[14] B. P. Jacob, S. Thankachan, S. Xavier, and E. M. Mohammed, "Effect of Gd3+ doping on the structural and magnetic properties of nanocrystalline Ni–Cd mixed ferrite," *Physica Scripta*, vol. 84, no. 4, 2011.

[15] R. Supriyanti, A. Chrisanty, Y. Ramadhani, W. Siswandari, "Computer Aided Diagnosis for Screening the Shape and Size of Leukocyte Cell Nucleus based on Morphological Image", *International Journal of Electrical and Computer Engineering (IJECE)*,Vol 8, No 1: February 2018.

[16] Adnan H. Ali,Ali N. Abbas, M. H. Hassan," Performance Evaluation of IEEE802.11g WLANsUsing OPNET Modeler", (AJER) Volume-02, Issue-12, pp-09-15.

[17] V. Be˙cyt ˇ e, K. Ma ˙ zeika, T. Rakickas, and V. Pak ˇ stas, ˇ *Mater. Chem. Phys*. 172, 6, 2016.